

Topological Excitations in Doped Spin Ladders

Yujoung Bai

National Creative Research Initiative Center for Superconductivity, Department of Physics, Pohang University of Science and Technology, Pohang, Kyungbuk 790-784, KOREA

We study low-energy magnetic excitations of doped spin-ladders, based on an effective Hamiltonian describing interactions of mobile spin and background spins. The helicity modulus against fluctuations in the ladder plane as well as out-of-the-plane are calculated in terms of the doping concentration, the leg number and interaction strengths in the ladder. The system has the lowest energy in spiral phases with out-of-plane mode in addition to the in-plane spirals. The doping range for spiral modes is computed and its relation to spin gap structure is discussed. Our results gives spiral order which can enhance existing antiferromagnetic order at certain doping or reduce it at very low density of holes. For odd-legged ladders, formation of spin gap at certain narrow doping range becomes possible via coupling of spirals and background spins. Our results of the doping range for gapped mode in odd-ladders agree well with those existing numerical studies.

I. INTRODUCTION

There have been numerous studies on long-range magnetic order in two-dimensional quantum systems, some of which employed mapping to (2+1)D non-linear sigma model(NLsM) [2] for the long-wavelength, low-energy states. Adding the effects of doped holes to 2D antiferromagnets, several works were done of the in-plane spiral modes by mean-field calculation [3] [17] [23] [21]. A couple of studies included the out-of-plane spirals generated in 2D systems, starting with t-J models [22] which incorporated the effects of mobile spin in magnetic background [1]. By "spiral" modes, we mean vortex rotations formed by background moments or long-wavelength excitations arising from fluctuations of staggered magnetization. In lower dimensions, some studies have been done for low-energy excitations in *undoped* spin ladders [6] [9] [14]. The ground state of even-legged ladders is known to be spin liquid(singlets), given strong to intermediate coupling –the exchange ratio being $J_{\perp} \geq J_{\parallel}$. The odd-legged ladders have even-parity channels and odd-parity channel due to the reflection symmetry, for example, three-leg ladders with 2 even-parity channel and 1 odd-parity channel. The spinon ground state of undoped three-leg ladders has the even-channel at the lowest and the odd-channel right above and the other even-channel on top [24]. The mean-field(MF) theory and numerical studies agree that the even-channel makes the spin liquid while the odd-channel makes the Luttinger liquid, before doping. After started doping, the hole spins tend to go into the even-channel, thus keeping the gapped mode just like even-ladders, much more likely than into the odd-channel. It has been mostly accepted that the "topological term" in the NLsM describing a *undoped* ladder is classified by the parity of leg numbers(n_l). The term is shown to be zero for undoped even-legged ladders and $2\pi S n_l$ for odd-legged ladders [7]. As for *doped* ones, there have been a couple of results which showed clear departure from this type of distinction, by numerical(DMRG) calculations [4] and by Lanczos calculations

along with mean-field theory [24]. In this paper, we focus on the low-energy topological excitations in doped ladders by analytical calculations. The meaning of the topological term for doped ladders will be discussed in section IV. "Doped" spin ladders consist of background spins (of Cu ions) and empty sites with residual spin interacting in the magnetic texture. The effective interaction between residual spins are antiferromagnetic, if they belong to different sublattices of any bipartite ladder sites [19]. New magnetic excitations arise from coupling of collective polarization and local magnetization, as the effective spin (of the hole) moves around the ladder sites. In the continuum limit, the distorted spin background induces non-zero "magnetic" flux due to quantum fluctuation. To see the spin response, the helicity modulus is calculated as an explicit function of doping rate, leg number, temperature and interaction strengths in spin ladders. By minimizing the total energy of the system, we find the range of hole concentration which favor the spiral mode, from the helicity modulus. Our results of the doping range for gapped mode in odd-ladders agree well with those existing numerical studies [24] [4], within reasonable range of interaction coupling in our model. Also, we determine how spiral modes enhances/suppresses AF order and the range for these effects.

II. THE MODEL AND THE PARAMETERS

In our study, we employ an effective Hamiltonian, based on the one made by Shraiman and Siggia for 2D magnets [1], which shows more explicitly the effective interactions related to gap generation, than other models do. The long-range Coulomb repulsion between holes is ignored. At half-filling, the low energy state has the commensurate Neel order. For the long-wavelength staggered spin state, the Neel vector is twisted, by $\alpha \frac{y}{L}$ around z-axis at the end of the ladder length L with respect to the first \hat{n} and by $\nu \frac{x}{(n_l-1)a_0}$ at the end of the ladder with n_l -leggs (with the lattice spacing a_0). When the mobile

spins are introduced upon doping, the Neel vector is allowed to rotate around y-axis as well, to derive all modes generated by collective polarization and quantum fluctuation. $\hat{n} = (\sin \theta \cos \phi, \sin \theta \sin \phi, \cos \theta)$. This is equivalent to twisting the spin quantization axis from site to site via appropriate transformation as done in some existing works [17] [23] [22].

$$H_{eff} = H_{NLsM} + \frac{1}{2} \left(\frac{\dot{y}\alpha}{L} \right)^2 + \frac{1}{2} \left[\frac{\dot{x}\nu}{(n_l - 1)a_0} \right]^2 - \tilde{g} \sum_{a,q} \hat{P}_a(q) \cdot \vec{j}_a(q) - g' \sum_{a,k} \cos k \bar{\Psi}_{k-\frac{2}{q}} \hat{\tau} \Psi_{k+\frac{2}{q}} \cdot \hat{m}(q) \quad (1)$$

where the magnetization current $\vec{j}_a(q) = \hat{n} \times \nabla_a \hat{n}$ and the dipole moment of the polarized background $\hat{P}_a(q) = \sum_k \sin k_a \bar{\Psi}_{k-\frac{2}{q}} \hat{\tau} \Psi_{k+\frac{2}{q}}$. The second and the third term is the rotational kinetic energy of the unimodular \hat{n} while the fourth term is the coupling between the induced polarization and spin current. The fifth term is effective interaction between the mobile spin and the surrounding magnetic moments. The subscript a stands for in-plane(IP) mode and out-of-plane(OP) spirals.

Taking only the slow component of the Neel vector in NLsM which describes the low-energy state of the background at half-filling, we approximate the local moment $\hat{m}(q) \simeq 2(-1)^{l+j-1} \hat{n} = \pm 2 \hat{n}$. The + sign is when the leg number(l) plus site number(j) is even while the - sign is for $(l + j)$ being odd. The wavevector of the mobile spin is related to the spiral wavenumber Q_a as $\langle \bar{\Psi}_{k-\frac{2}{q}} \Psi_{k+\frac{2}{q}} \rangle \approx Q_a \sin k_a$. Thus, one of the effective interaction term in H_{eff} producing the IP spiral becomes

$$\begin{aligned} V_g \simeq & -\tilde{g} \sum_{q,k} \sin k \bar{\Psi}_{k-\frac{2}{q}} \hat{\tau} \Psi_{k+\frac{2}{q}} \cdot \hat{n} \times \nabla_\phi \hat{n} \\ & = -\tilde{g} \sum_k Q \sin^2 k [-\sin \theta \cos \theta (\cos \phi + \sin \phi)] \\ & \rightarrow -\tilde{g} \sum_k Q \sin^2 k [\cos(Q_x/2) - \cos(Q_y/2)] \quad (2) \end{aligned}$$

The last equation comes from identifying the components of incommensurability wavevector $\vec{Q} = (Q_x, Q_y)$ varying from site to site, as given by the twisted (spherical) angles ϕ and θ in the equation above. For IP spiral mode, above V_g is dominant over the other effective interaction $V_{g'}$.

The spiral wavevector \vec{Q} is shown in Fig. 1 and Fig. 2.

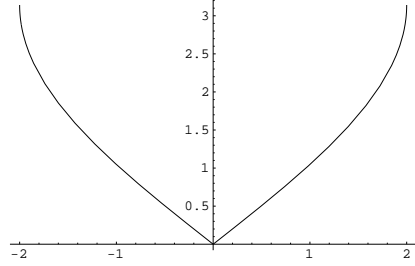


FIG. 1. Spiral wavevector Q_y vs. Q_x for $0 < \phi < \pi$. Q reaches the maximum at $Q_x = 0$, which indicates the gap formation along the y -direction. In real space, this implies triplet formation along the ladder direction.

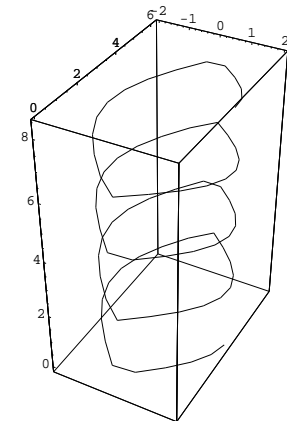


FIG. 2. Spiral wavevector shown for $0 < \phi < 8\pi$. For IP mode, the up-direction in this figure corresponds to the rung direction of ladders.

In the ladder plane, the (Q_x, Q_y) has a symmetry similar to a d-wave. The effective propagation in real space is along the rung direction of the ladder. This mode is equivalent to the “transverse” mode [17] or to the “stripe” phase [21] as termed in other works for 2D systems [3]. The doping range for the spiral order to occur is computed from the helicity modulus against in-plane(IP) twisting. The spiral wavenumber Q is proportional to the doping rate, though a more precise form is computed in Section. IV. For the purpose of calculating the helicity modulus, we use $Q \approx \delta \frac{t_\perp}{J_\perp}$ for IP mode and $Q \approx \delta$ for out-of-plane(OP) spirals.

For IP mode, the effective Hamiltonian density is given

$$\begin{aligned} H_{eff} = & (\partial_a \psi)^2 + \frac{1}{2} \left(\frac{\dot{y}\alpha}{L} \right)^2 + \frac{1}{2} \left(\frac{\dot{x}\nu}{(n_l - 1)a_0} \right)^2 - \\ & 2\tilde{g}\delta \frac{t_\perp}{J_\perp} \{ \cos \phi (\cos \phi + \sin \phi) \} \sin^2 k \\ & \pm 2g'\delta \frac{t_\perp}{J_\perp} \cos \phi \sin k \cos k \quad (3) \end{aligned}$$

III. HELICITY MODULUS AND SPIRAL MODES

The free energy per unit area of the ladder plane is

$$\begin{aligned}
F &= -\frac{1}{\beta} \ln \text{Tr} \exp[-\beta H_{\text{eff}}] \\
&= -\frac{1}{\beta} \ln \left[\frac{2\pi(n_l - 2)}{a_0^2(n_l - 1)} \right] + \beta \left[\frac{1}{2} \left(\frac{\dot{y}\alpha}{L} \right)^2 + \frac{1}{2} \left(\frac{\dot{x}\nu}{(n_l - 1)a_0} \right)^2 \right] \\
&\quad + \frac{1}{2\beta} \ln [2\beta^2 \{1 + A \cos \phi (\cos \phi + \sin \phi)\}] \\
&\quad - \frac{\beta B^2 \cos^2 \phi}{4\{1 + A \cos \phi (\cos \phi + \sin \phi)\}} \tag{4}
\end{aligned}$$

where $A = -2\tilde{g}\delta \frac{t_\perp}{J_\perp}$, $B = -2g\delta \frac{t_\perp}{J_\perp}$ and $\beta = 1/k_B T$. The subscript \perp refers to those along the rung direction while \parallel is for those in the chain(ladder) direction.

The spin wave velocity for doped ladders is derived from mapping the unit ladder cell (repeated regularly as defined by the density of empty sites) to NLsM. First, we write the variation of the Neel vector in NLsM [16], $\delta\hat{n}(jr) \simeq \hat{n}_1(jr) - \hat{n}_2(jr + \frac{r}{2})$, where $r = 1/\delta$. In the long wavelength continuum limit, the coherence length \gg the ladder width($a n_l$) and using $\vec{m} \cdot \partial_\tau \vec{m} = 0$ and $\vec{m} \cdot \delta \vec{m} = 0$, the Hamiltonian is given

$$H_{\text{NLsM}} = \frac{1}{2g} *$$

$$\int_0^\beta \int \left[\frac{1}{v_s} (\partial_\tau m)^2 + v_s (\partial_a m)^2 - \frac{\theta}{4\pi} (\partial_a m)^2 \right] d^2 r d\tau \tag{5}$$

where the coupling from NLsM includes now the doping effect $g = [(1 - \delta)n_l S]^{-1} \left(1 + \frac{J_\perp}{2J_\parallel}\right)^{\frac{1}{2}}$, assuming low density of empty sites. Then, the spin wave velocity is collected from the prefactor, $v_s = 2S J_\parallel \left(\frac{1-2\delta}{1-\delta}\right) \left(\frac{1+J_\perp}{2J_\parallel}\right)^{\frac{1}{2}}$. The θ -term in H_{NLsM} is the “topological” term. As for 2D systems (without any hedgehogs), it is known that the topological term is zero, regardless the spin number or the configurations of lattice sites [10] [11] [12] [13]. In Section VI, we discuss the different role of this term in doped ladders.

The coupling in the effective interaction($V_{g'}$) is found from relating the hole density to the induced (collective) polarization $\langle P_{g'} \rangle$ and the incommensurability wavenumber Q of the spiral mode. From mean-field approximation as done in Section IV and $\langle V_{g'} \rangle \simeq 2g' Q \ln[2(n_l - 1)]$, $\langle P \rangle \simeq g' Q(n_l - 1)L/16\pi^2 a_0$, we estimate the coupling

$$g' \approx \frac{J_\perp Q}{\langle P \rangle} \approx \frac{32a_0\pi^2 \ln[2(n_l - 1)]\delta J_\perp}{L(n_l - 1)} \tag{6}$$

where L is the length of unit ladder cell, which decreases as hole density increases. The other coupling \tilde{g} can have different values depending on the interaction strengths and the doping rate in physical ladders. The order of magnitude can be estimated from renormalized coupling of the NLsM(σ); $1/\tilde{g} = 1/g_\sigma + \text{Tr} \frac{1}{[k^2 + V(\tilde{g})]}$. For instance, given the most realistic interaction strengths in cuprate ladders $\frac{t_\perp}{J_\perp} = 5$, $\tilde{g} \sim 1$ with $\delta = 0.1$, while it becomes a much greater number with a higher δ .

The helicity modulus against the in-plane fluctuations is computed from above free energy

$$\begin{aligned}
\mathfrak{R}_{\text{IP}} &= \frac{v_s}{2} \left| \frac{\partial^2 F}{\partial \phi^2} \right|_{\phi=0} \\
&= \left(\frac{1-2\delta}{1-\delta} \right) \frac{(\tilde{g}\delta t_\perp)^2}{\beta J_\perp (1-2\tilde{g}\delta \frac{t_\perp}{J_\perp})^2} \left(1 + \frac{J_\perp}{J_\parallel} \right)^{\frac{1}{2}} * \\
&* \left[1 - \frac{(128\pi^2\beta \ln[2(n_l - 1)]a_0\delta^2 t_\perp)^2}{(n_l - 1)^2(2\tilde{g}\delta \frac{t_\perp}{J_\perp} - 1)} \right] \tag{7}
\end{aligned}$$

This is an explicit function of the doping concentration δ , leg number n_l , temperature and the interaction strengths in the ladder t_\perp , J_\perp and J_\parallel .

Though the results have temperature dependence, the model is more meaningful in low temperature and low doping regime. Figure 3-4 are 3D (surface) plots of the in-plane helicity modulus(HM) versus doping rate and temperature. The common features are (i) that the HM diverges at certain doping rate $\delta = 1/(2\tilde{g}\frac{t_\perp}{J_\perp})$, (ii) that the sudden jump is followed by sharp decrease in HM to negative values, (iii) that the flat plateau is over wide range of doping and temperature, (iv) that another range for sharp increase of HM is at $0.8 \leq \delta \leq 0.9$.

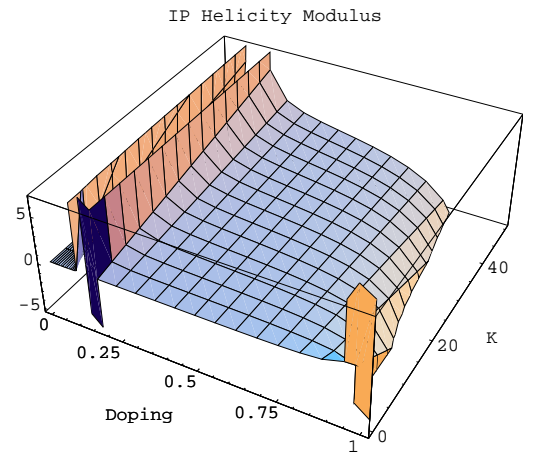


FIG. 3. IP helicity modulus(HM) for 2-leg ladder with $\tilde{g} = 1$, $t_{\perp} = 0.2$ eV and $J_{\perp} = 0.04$ eV. The temperature is given in K. When HM becomes negative, spiral modes are formed as shown for $0.1 < \delta < 0.2$. The diverging HM at $\delta = 0.1$, followed by drastic decrease to negative values and by flat region, imply presence of spin gap. The sharp increase at higher $\delta \geq 0.8$ with subsequent negative region indicates another window of spiral phase.

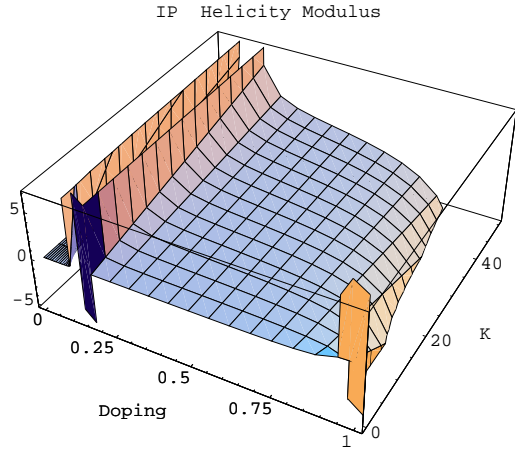


FIG. 4. IP helicity modulus(HM) for 3-leg ladder. The characteristics are same as those for 2-leg ladders, though precise values are a bit different, due to the leg-number dependence in the couplings (g). As leg-number increases, the doping regime for IP spiral mode is reduced.

In Fig. 3, HM for 2-leg ladders with the typical $\frac{t_{\perp}}{J_{\perp}} = 5$ and $\tilde{g} = 1$, diverges at $\delta = 0.1$. The spin liquid ground state acquires excited triplets upon doping. When the hole density reaches a certain level, intrachain pair formation becomes substantial as well, which makes the whole system very stiff. The diverging modulus followed by drastic decrease as well as flattening over wide range, indicate presence of spin gap, since the HM(stiffness) goes as the inverse of spin susceptibility. In the region of negative HM, the system releases spiral modes to lower the energy. This accompanies reduction of spin gap sizes in those ladders with existing spin gaps inherited from undoped systems. As doping increases further, there is another sharp increase in HM at very low temperatures. This is due to quantum fluctuation of the staggered magnetization. Resultantly, bound-states among spirals of opposite chirality (soliton and anti-soliton pair) may form. The spin quantum number would be 1 (or integers) for this new type of “condensate”. This is reminiscent of “pseudogap” structure in higher dimensional systems. The spiral modes can put a pair of spins- (one in up-sublattice and the other down-sublattice) into a level *in* the gap. Thus, the (short-range) AF order of spin liquids can lose it at certain doping regime. At higher \tilde{g} which is also physically feasible, the spiral phase is absent at low doping, though the gap features still remain. In this case, the background magnetic order is not likely

to develop a new phase at low doping regime.

Shown in Fig. 4 for 3-leg ladder, the possibility of generating spin gap in odd-ladders exists at around $\delta = 0.1$, if actual $\tilde{g}=1$ in physical systems. To have another window of gap formation in odd-ladders, either the temperature needs be very low $T \leq 5K$ or the effective coupling \tilde{g} between the polarization and the spin current be very small. In our estimate for realistic value of this coupling, it is of order of 1, rather than order of 0.1. For $\tilde{g} \geq 1$, gap formation around $0.8 \leq \delta \leq 0.9$ at high doping regime may occur at temperatures near 0. For $\tilde{g} \leq 1$, gap formation at small doping $\delta < 0.1$ is possible. Experimentally, it may be difficult to provide precisely such narrow range of doping in order to verify formation of spin gap in doped odd-ladders. From the plots, the region where the HM becomes negative is commonly $2\tilde{g}\frac{t_{\perp}}{J_{\perp}} < \delta < 0.5$ at $T \leq 5K$. These allow spiral phases for all ladders. The characteristics are repeated for ladders with any number of legs, though precise values are a bit different, due to the leg-number dependence in g . As leg-number increases, the doping regime for IP spiral mode is reduced. Since the even-parity channels in odd-ladders are dominant over the odd-parity channels, the added(effective) spins tend to be in the even-channels. Given the attractive potentials provided by V_g 's in our model, binding of the spins in the odd-channel and the spirals(solitons) yield an energy gap. This gives rise to a gapped phase at $\delta \geq \delta_{\text{spiral}}$ in odd-ladders(see Section III), with all channels participating. Existing interpretation of gap generation in odd-ladders by White *et.al.* uses the idea of domain walls formed by competition between the kinetic energy and the exchange energy. In our picture, domain walls can be interpreted as areas of the spiral vortices with different spiral wavenumber or different chiralities (see Section VI). Alternative understanding has been given with proximity effect to the gapped mode of the even-channel, which enhances the pairing within the odd-channel [24] [18].

For out-of-plane(OP) mode, the effective spin $\hat{\tau}$ of the empty site is taken along \hat{z} . The effective Hamiltonian for OP contribution is

$$H_{\text{eff}} = (\partial_a \psi)^2 \pm 2g\delta \sin k \cos k \cos \theta \quad (8)$$

The free energy per unit area along the \hat{z} is

$$F = \frac{-1}{\beta} \left[\ln\left[\frac{2\pi}{\beta}\right] + 2(g\cos\theta\delta\beta)^2 \right] \quad (9)$$

The helicity modulus(HM) against the out-of-plane twisting is

$$\begin{aligned} \mathfrak{R}_{\text{OP}} &= \frac{v_s}{2} \left| \frac{\partial^2 F}{\partial \theta^2} \right|_{\theta=0} = \\ &- 2\beta \left(\frac{32\pi^2 \ln[2(n_l - 1)]}{(n_l - 1)} \right)^2 \left(\frac{1 - 2\delta}{1 - \delta} \right) \delta^4 J_{\perp}^3 \left(1 + \frac{J_{\perp}}{J_{\parallel}} \right)^{\frac{1}{2}} \end{aligned} \quad (10)$$

Figures 5-6 show the plotted HM as functions of hole concentration and temperature. At low doping, the dependence on temperature is negligible.

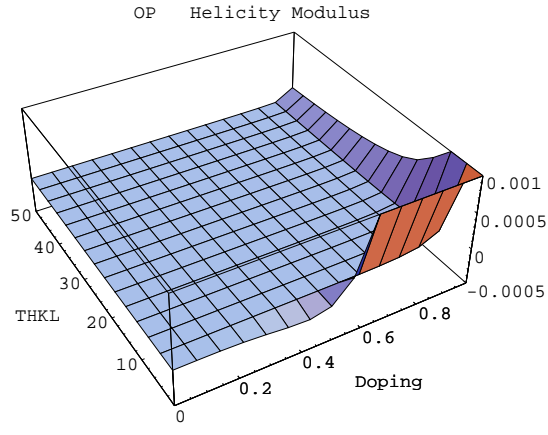


FIG. 5. OP helicity modulus(HM) for 2-leg ladder. The temperature is given in K. Spiral mode coming out-of-plane is formed in the doping range $0.2 \leq \delta < 0.6$. Beyond this doping, the HM increases sharply at low temperatures, suggesting bound states formed of OP spirals.

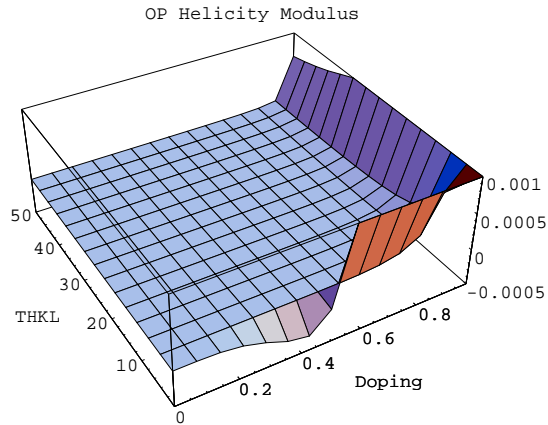


FIG. 6. OP helicity modulus(HM) for 3-leg ladder. OP spiral mode is formed at doping range slightly higher than that for 2-leg ladders. Overall features are common for ladders with more number of legs, given the weaker dependence of the HM on leg-number than the dependence on doping or temperature.

Other features are determined most dominantly by the coupling g' parameter. For a exchange ratio of $J_{\perp} = 2J_{\parallel}$, the results show the formation of OP spiral mode around $0.2 \leq \delta < 0.6$ for 2-leg ladders and $0.3 \leq \delta < 0.7$ for 3-leg ladders. In both 2-leg and 3-leg ladders, there are sharp increases in the HM around $\delta = 0.6$ for $T < 15K$, making OP spiral robust. At very high hole density beyond this δ , the peaked modulus indicates forming of bound states of OP spirals with opposite chirality. For such phases of bound spirals(soliton-antisolitons), we may call it "spiral

liquid" or "soliton liquid" (termed by Haldane). These features are same for ladders with more number of legs, regardless the parity of leg number. The HM(stiffness) decreases as temperature increases at high doping ranges for all ladders.

IV. DOPING CONCENTRATION FOR SPIRAL PHASE

The Fermi distribution function $n^{\pm} = \exp[\beta(\varepsilon_k \mp \tilde{g} Q \sin k - \mu)] + 1$ gives $n^+ - n^- \approx 2\beta\tilde{g} Q \sin k$, at low T . From minimizing the Hamiltonian H_{eff} with respect to a mean-field Q [1], the self-consistency condition gives $Q = \frac{\tilde{g}}{\Re} \sum_k \sin k (n^+ + n^-) \simeq \frac{2\tilde{g}\beta}{J} \sum_k \sin k (\mu - \varepsilon_k)$ at low T . Then the mean effective interaction terms are

$$\langle \tilde{V}_g \rangle + \langle \tilde{V}_{g'} \rangle$$

$$\simeq -\frac{\tilde{g}^2}{\Re} \sum_k \sin^2 k (2\beta\tilde{g} Q \sin k)^2 + \frac{1}{2} \Re Q^2 \quad (11)$$

The $\langle H_{MF} \rangle$ becomes positive when the helicity modulus \Re becomes negative, which makes the system unstable. So, the system releases the torsional momenta. That is, the spiral phase with uniform wavenumber (throughout the system) is favoured when $\Re < 0$. From \Re_{IP} in eqn.(7) and for realistic parameter regimes of J , t and n_l , we find the doping range for spiral phase

$$\frac{J_{\perp}}{2\tilde{g}t_{\perp}} \leq \delta < \frac{1}{2} \quad (12)$$

Above holds for ladders with any number of legs, which agrees with what are shown in our plots of the helicity modulus(HM). As for the OP HM, it is negative over rather wide range of doping at low temperatures. Therefore, the system under this doping (making OP HM negative) favours to have both modes of spirals -IP and OP. The result indicates very interesting physics of spin gap structures and HM(stiffness). At a given temperature, the higher the stiffness, the lower the spin susceptibility. Comparing cases of different gap sizes, the greater the spin gap, the lower the susceptibility at the temperature. That is, increasing HM for a system means increasing gap size, which can give rise to higher kinetic energy. This is released as spiral mode with smaller pitches (inversely proportional to the wavenumber) which may impart more kinetic energy to charge transport.

The spin coherence length is computed when the HM is zero from eqn. (7), by putting $L = \xi$.

$$\xi \simeq \frac{128a_0\pi \ln[2(n_l - 1)]\delta\beta J_{\perp}}{(n_l - 1)[2\delta\tilde{g}t_{\perp}/J_{\perp} - 1]^{1/2}} \quad (13)$$

When the incommensurate spin state is stable in the regime of positive HM, it is possible to gather the (hole)

spins along valleys of the spiral wavevector. This may result in “phase separation” of hole-rich region and no-hole region [17] [15]. Though more study is needed for the process of phase separation, we can estimate the doping range for this. Luttinger liquid phase is believed to be adjacent to spiral phase [28]. As for spin ladders with even number of legs, the upper limit of doping for the Luttinger liquid phase is $J/2t\tilde{g}$. The lower limit would be around $J/4t\tilde{g}$, considering the realistic interaction strengths t , J in CuO ladders.

In our results, there is no transition like Kosterlitz-Thouless(KT) transition in 2D, since there is no strong size dependence and no plateau in the stiffness around any particular temperatures. Though there are size dependent terms in the expression of the HM, these are rather weak. If there was KT transition, the spin gap function would have the form of $\sim \exp[-a/J^{\frac{1}{2}}]$. Calculated spin coherence suggests that the gap function has a different form from this, due to the doping effect.

As far as the helicity modulus, ladders with even/odd-number of legs do not have differing signs, since the factor $\ln[2(n_l - 1)]$ does not distinguish the parity in n_l . This is the difference from the result on 1D spin chains which distinguish the parity, but analogous to 2D systems which do not differentiate the spin quantum number being integer or half-odd integer.

V. PARITY IN ODD-LEGGED LADDERS

Our result shows that formation of spin gap becomes possible at certain doping rate even in odd-ladders by allowing the spiral phase. To examine the relation of leg-number and gapped mode further, we consider the wavefunction in ladders with any number of legs. The spin state at ladder sites would be composed of Slater determinant of single-spin wavefunction. By relating the spin at site $j+1$ and at leg l to the one at the initial point $j = 1$ and $l = 1$, the phase factors in the wavefunction at the end of the boundary is given $S_l^{\pm}(j+1) = \exp[i(\phi(j) + \phi(l))]S_1^{\pm}(1)$ [8]. The wavefunction from Jordan-Wigner transform is written

$$\Psi_l(j) = S_l^-(j)(-1)^l \exp[i\pi \sum_{a=1}^{l-1} S_a^z(j) + \frac{1}{2}]. \quad (14)$$

When the number $n_l + n$ is odd, the wavefunction has an additional sign factor compared to that of the case when the number $n_l + n$ is even. $\Psi_l(n+1) = \pm \exp[-i\phi]\Psi_1^1$, where n is the site number in the block of the system. Due to the fact that our systems are ladders with finite number of legs (and/or negligible coupling between ladders consisting the bulk), above boundary condition is legitimate. That is, the meaningful parity in ladders is that of (leg number plus site number), instead of the leg number alone. We interpret the “+” or “-” sign as the chirality associated with the (winding) orientations of spirals, having arisen from the presence of

two sublattices(up or down-spin). So, the ground state in *odd-ladders* is degenerated allowing spiral modes with different chiralities at different ladder regions, thus satisfying Lieb-Mattis-Shulz theorem. This means that gapped mode is possible in odd-ladders as well as in even-ladders. This is the same result as found by previous study on odd-ladders [19]. Our result of doping rate for the gapped mode in odd-ladders ($\delta_{\text{spiral}} = 0.1$ for $\tilde{g} = 1$) is close to the result by Rice et. al. [24] who found the $\delta_c \geq 0.13$. If the coupling $\tilde{g} < 1$ in physical ladders, the DMRG result of $\delta_c \geq 0.06$ by White et. al [4] is comparable as well. In our picture, there is interplay between effective interaction strengths and hole concentration, giving the coupling g vary consequently.

VI. ANTIFERROMAGNETISM AND SPIRAL PHASE

So far, we restricted the spiral winding number (w) to 1, to ensure the spinor wavefunction to be periodic (instead of anti-periodic). The staggered spin flux(chirality) in continuum limit is $2\pi w$. In terms of the Neel vector at bipartite ladder sites, the winding number is given $[\hat{n}_1 \cdot \hat{n}_2 \times \hat{n}_3 + \hat{n}_1 \cdot \hat{n}_3 \times \hat{n}_4 - \hat{n}_1 \cdot \hat{n}_2 \times \hat{n}_4 - \hat{n}_2 \cdot \hat{n}_3 \times \hat{n}_4]$. If the systems were undoped ladders described by NLsM, the w would be equal to the topological term. This gives the solid angle subtended by the Neel vectors or the Berry phase acquired by the Neel vector while traversing around the path in spin space. $2\pi S w = w\pi$ for $S = 1/2$ gives the staggered “magnetic” flux [25] [26]. Allowing the spiral modes, the winding number need not be integers. This implies that the “topological” term in *doped* ladders do not simply determine their classes by the leg numbers.

The induced field acting as twisted boundary would affect the magnetic ordering in ladders. To see whether spiral modes compete with antiferromagnetism in *ladders* or not, we rewrite the Neel vector including the winding number for IP spiral. $\hat{n} = (\sin \theta \cos(w\phi), \sin \theta \sin(w\phi), \cos \theta)$. Then, the effective interaction term with \tilde{g} is given including the winding number, coming from the gradient of \hat{n} , $V_g \sim -\pi^2 w \tilde{g} \delta$. This can provide attractive potential [20] between the polarised spin and the spin current if the w is positive. To maintain the attractive potential between the spin texture and the spiral(soliton), w is chosen to be of the chirality “+”. This would result in destroying the AF order of background spins. However, there is another interaction term $V_{g'}$ in our effective Hamiltonian, which does not depend on the winding number. This contribution can be greater in length scales of a few lattice constant, though it decreases as the doping decreases and/or the leg number increases. In cases of very low hole density (a few percent) and many number of legs, it is possible that the V_g wins to reduce the AF order.

A known result by Arrigoni et. al. on spiral order from

2D Hubbard model with one term $(\epsilon - \mu) \sum_{i\sigma} C_{i\sigma}^+ C_{i\sigma}$ added shows that there is one spiral mode (“transverse”) in which AF order is *enhanced*. The other spiral mode can enhance ferromagnetic order of the background. Another work by Mori et. al. on 2D $t - J$ model also show two similar spiral phases. As for doped *ladders* which started with commensurate Neel order at half-filling, our result show that the whether spiral modes reduce or enhance the AF order depends directly on the hole density. Only at very low doping regime (a few percent), spiral order suppresses antiferromagnetism. It is due to that the effective interactions $V_{g\uparrow}$ and $V_{g\downarrow}$ can compete in some doping regime while they conspire in other hole density. As pointed out in Section II about the incommensurability wavevector, our model yields effectively, one spiral mode in the ladder plane (with the wavevector directed along the rung direction), the other mode coming out-of-plane.

In summary, due to the hole motion distorting the spin texture in doped ladders, quantum fluctuation of the staggered magnetization yields new type of excitations. In continuum limit, long-range spiral modes arise and give the helicity modulus vary as the doping rate, temperature, leg number and interaction strengths. The spiral modes can put magnons (one spin in up-sublattice and the other down-sublattice) into a level in the gap. The spin gap is reduced in even-ladders while it can be generated in odd-ladders, depending on hole density. Since the even-parity channels in odd-ladders are dominant over the odd-parity channels, the added spins tend to be in the even-channels. Thus, in the begining of doping, the even-channels give the spin gap as spin liquids of undoped ladders. Given the attractive potentials provided in our model, the spin current in the odd-channels tend to make bound states with the spirals in the even-channel. The enhanced pairing brings out the gapped Luther-Emery phase at $\delta \geq \delta_{\text{spiral}}$ in odd-ladders. Our results of the doping range for gapped mode in odd-ladders agree well with those existing numerical studies. Antiferromagnetism can be enhanced over substantial doping range via allowing spiral modes. At very low doping of few percentage, spiral modes promote ferromagnetism. In this paper, we showed analytically, generation of spin gaps in odd-ladders and the explicit relation between magnetic orders and topological excitation (spiral modes). In our forthcoming study, we are to examine whether the spiral phase enhances superconducting transition or suppresses via tunneling of solitons.

ACKNOWLEDGMENTS

This work is supported by Creative Research Initiatives of the Korean Ministry of Science and Technology.

- [1] B. Shraiman and E. Siggia, Phys. Rev. Lett. **62**, 1564 (1989)
- [2] S. Chakravarty, B. Halperin and D. Nelson, Phys. Rev. B**39**, 2344 (1989)
- [3] A. Auerbach and B. E. Brown, Phys. Rev. B**43**, 7800 (1991)
- [4] S. R. White and D. J. Scalapino, Phys. Rev. B**55**, 14701 (1997), Phys. Rev. B**57**, 3031 (1998)
- [5] E. Dagotto *et. al.* Phys. Rev. B**45**, 5744 (1992)
- [6] D. Sénéchal, Phys. Rev. B **52**, 15319 (1995)
- [7] G. Sierra, J. Math. Phys. A. **29**, 3289 (1996)
- [8] D. Loss and D. Maslov, Phys. Rev. B**74**, 178 (1995)
- [9] S. Dell’Aringa *et. al.* Phys. Rev. Lett. **78**, 2457 (1997) and the references therein.
- [10] F. D. M. Haldane, Phys. Rev. Lett. **61**, 1029 (1988)
- [11] E. Fradkin and M. Stone, Phys. Rev. B**38**, 7215 (1988)
- [12] T. Dombre and N. Read, Phys. Rev. B**38**, 7181 (1988)
- [13] L. B. Ioffe and A. I. Larkin, Int. J. Mod. Phys. B. **2**, 203 (1988)
- [14] B. Normand, J. Kyriakidis and D. Loss, cond-mat/9902104
- [15] E. Orignac and T. Giamarchi, Phys. Rev. B**56**, 7167 (1997)
- [16] T. Fukui *et. al.* Phys. Rev. B**56**, 2530 (1997)
- [17] E. Arrigoni and G. C. Strinati, Phys. Rev. B**44**, 7455 (1991)
- [18] V. J. Emery, S. A. Kivelson and O. Zachar, Phys. Rev. B**56** 6120 (1997)
- [19] M. Sigrist and A. Furusaki, J. Phys. Soc. Jpn. **65**, 2385 (1996)
- [20] S. John and A. Golubentsev, Phys. Rev. B**51**, 381 (1995)
- [21] H. Mori and M. Hamada, Phys. Rev. B**48**, 6242 (1993)
- [22] M. Hamada, H. Shimahara and H. Mori, Phys. Rev. B**51**, 11597 (1995)
- [23] C. L. Kane *et. al.* Phy. Rev. B**41**, 2653 (1990)
- [24] T. M. Rice *et. al.* Phy. Rev. B**56**, 14655 (1997)
- [25] G. Baskaran, Phys. Rev. B**63**, 2524 (1989)
- [26] P. Lee and N. Nagaosa, Phys. Rev. B**46**, 5621 (1992)
- [27] J. M. Kosterlitz and D.J. Thouless J. Phys. C **6**, 1181 (1973)
- [28] Y. Bai and S.-I. Lee, cond-mat/9906302